Desalination and Water Treatment
www.deswater.com

doi: 10.5004/dwt.2020.26036

198 (2020) 163–169
September

Selective ion adsorption with pilot-scale membrane capacitive deionization (MCDI): arsenic, ammonium, and manganese removal

Edgardo E. Cañas Kurz[a,b,c,*], Ulrich Hellriegel[a,b,c], Vu T. Luong[d,e], Jochen Bundschuh[f,g], Jan Hoinkis[a,f]

[a]*Center of Applied Research, Karlsruhe University of Applied Sciences, Moltkestr. 30, 76133 Karlsruhe, Germany, Tel. +49 (0)721 925 1367; email: edgardo.canas_kurz@hs-karlsruhe.de (E.E. Cañas Kurz), Tel. +49 (0)721 9251365; email: ulrich.hellriegel@hs-karlsruhe.de (U. Hellriegel), Tel. +49 (0)721 9251372; email: jan.hoinkis@hs-karlsruhe.de (J. Hoinkis)*
[b]*Laboratory of Industrial and Synthetic Organic Chemistry (LISOC), Department of Chemistry and Chemical Technologies, University of Calabria, Via Pietro Bucci 12/C, 87036 Arcavacata di Rende (CS), Italy*
[c]*Institute on Membrane Technology, National Research Council (CNR-ITM), Via Pietro Bucci 17/C, 87036 Arcavacata di Rende (CS), Italy*
[d]*Department of Mechatronics and Sensor Systems Technology, Vietnamese-German University, Le Lai Street, 822096 Binh Duong Province, Vietnam*
[e]*Department of Separation Science, School of Engineering Science, Lappeenranta-Lahti University of Technology, Sammonkatu 12, 50130 Mikkeli, Finland, Tel. +358 (0)46 6385791; email: vu.luong@lut.fi (V.T. Luong)*
[f]*School of Civil Engineering and Surveying, University of Southern Queensland, West Street, Toowoomba, 4350 Queensland, Australia, Tel. +61 7 4631 2694; email: jochenbundschuh@yahoo.com (J. Bundschuh)*
[g]*UNESCO Chair on Groundwater Arsenic within the 2030 Agenda for Sustainable Development, University of Southern Queensland, West Street, Toowoomba, 4350 Queensland, Australia*

Received 24 January 2020; Accepted 27 April 2020

ABSTRACT

A pilot-scale membrane capacitive deionization (MCDI) unit was used for the selective removal of arsenic (up to 300 µg L^{-1} As(V)), ammonium (25 mg L^{-1} NH_4^+), and manganese (6 mg L^{-1} Mn^{2+}) in experiments with brackish water. Tests were carried out using a commercially available MDCI module and different initial salt concentrations (total dissolved solids, TDS = 0–2 g L^{-1} NaCl) to investigate the removal capacity and behavior of the MCDI unit with different operational parameters such as applied current, voltage, flow rate, and experimental settings such as pH. Selectivity and adsorption behavior is described and a comparison with lab-models is presented to validate the results obtained in real-life scale and application. While the adsorption capacity of the module decreased with higher TDS, specific ion adsorption improved with ionic mobility and greater ion charge. Removal of NH_4^+ and Mn^{2+} at given concentrations was significantly higher than for As(V) but rejection of As(V) could be significantly increased (30%–89.5%) by raising the initial pH value above its $pK_a = 6.94$. Depending on selected operational settings and feed water characteristics, the total energy consumption of the MCDI unit (only electrodes) ranged between 0.89 and 2.74 kWh m^{-3} with an overall optimum at <1 kWh m^{-3}.

Keywords: Electrosorption; Ion mobility; Groundwater remediation

---

* Corresponding author.

1. Introduction

1.1. Background

In many rural areas, groundwater is the only viable way to provide safe and consistent drinking water. However, about 600 million people worldwide currently inhabit low-elevation coastal zones that are affected by progressive salinization [1,2]. Besides salinization problems, high concentrations of geogenic arsenic (As) are found in groundwater of some regions in Southeast Asia [3], Bangladesh [4], West-Bengal (India), [5,6], China [7], and many other areas [8,9]. In confined aquifers with a reducing hydrogeochemical environment, the mobilization and release of geogenic bound As into the groundwater is a result of the reductive dissolution of both iron (Fe) and manganese (Mn) oxides [7,10]. The formation and speciation of As in a solution depend strongly on the pH and redox conditions. In reducing environments, arsenite (As(III)) is present as uncharged arsenious acid (H_3AsO_3) below pH 9.2, while arsenate (As(V)) is found in ionic form as $H_2AsO_4^-$ ($pK_a = 2.22$) or as bivalent ion $HAsO_4^{2-}$ ($pK_a = 6.98$) around neutral pH [11].

In addition, some of the regions with predominantly high As levels also show patterns of elevated concentrations of phosphate (PO_4^{3-}), dissolved organic carbon (DOC), and particularly, ammonium (NH_4^+) [12,13] and manganese (Mn^{2+}) [14,15]. A holistic groundwater remediation approach must therefore also consider the removal of these contaminants. Iron, which is also related to As in groundwater, was removed upfront by precipitation in order to avoid clogging of the MCDI unit. A detailed study on iron removal was reported by Canas Kurz et al. [16].

1.2. Objectives

The aim of this study is to investigate the feasibility of membrane capacitive deionization (MCDI) as a solution for the removal of As(V) from brackish groundwater for the first time using a pilot-scale plant. With both rural and urban populations affected by groundwater salinization and alarming levels of As, Mn, and NH_4^+, the study includes the elimination of Mn^{2+} and NH_4^+ for the production of drinking water quality. The study focuses on the experimental investigation of operational parameters (e.g., voltage, current, volume flow) and experimental conditions (e.g., pH) to evaluate the adsorption and removal efficiency of the selected ions.

2. Materials and method

A commercial MCDI unit consisting of an electrode module (CapDI, Voltea) with 75 electrode cells was used to evaluate the total salt rejection and the specific removal efficiency of As(V), Mn^{2+}, and NH_4^+ in natural (tap) and synthetic water. Each cell consisted of symmetrical active carbon electrodes (ca. 250 μm thickness) on graphite electrodes as current collectors, separated by a cellulose spacer (ca. 650 μm thickness). Aminated anion exchange membranes (AEM) and sulfonated cation exchange membranes (CEM) were placed in front of the anodes and cathodes, respectively. The total cell area was 1.78 m^2 with a total module volume of 2.9 L.

Model water for the tests with As was prepared using an As(V)-standard solution (Merck, Germany) (0–200 μg L^{-1}). Ammonium and Mn^{2+} were added in the form of ammonium chloride (NH_4Cl) and manganese sulfate ($MnSO_4 \cdot H_2O$) for each test, respectively. Sodium chloride was added for the different total dissolved solids (TDS) concentrations (0, 0.5, 1.0, and 2.0 g L^{-1} NaCl). Experiments were carried with DI and tap water. Table 1 summarizes the water parameters of model water.

Total inorganic arsenic (t-As) concentrations were measured using the hydride technique with atomic absorption spectrophotometry (AAS ContrAA, Analytik Jena, Germany). Measurements of manganese were carried out using the AAS flame technique. Ammonium concentrations were measured with ion chromatography (IC, Metrohm Compact, Germany) using a Metrosep C4 150/4.0 column. Sample measurements were repeated at least twice and samples were kept according to EN ISO 5667-3. Electrical conductivity of the solution was monitored using a portable pH-meter (WTW 315i) as reference for TDS (NaCl) measurements.

Experiments were conducted to investigate the effect of different operational settings on the removal efficiency at the pilot scale such as diluate flow and electric current. The module was run on constant current with reversed voltage during the discharge phase. Table 2 shows the cycle parameters set for charge and discharge phases for the two operation modes: low-energy operation (mode A) and high-performance configuration (mode B). In mode B, applied current and volume flow during the charge and pre-charge phase were, respectively, increased (18.1–45 A) and lowered (1.0–0.25 L min^{-1}) to improve total removal efficiency. Charge and discharge cycle times were kept constant for all experiments. Each experiment ran between 1 and 4 h with a maximum flow of 1.0 L min^{-1} and maximum water recovery of 81%.

The operational settings in mode A for all the single-pass experiments were selected based on previously experimentally determined configurations with the MCDI unit for optimum specific energy consumption SEC (kWh m^{-3}) in experiments with 1,000 mg TDS L^{-1}. Values for specific

Table 1
Model water composition and average tap water quality

Parameter	Concentration(s)
Arsenic As(V), μg L^{-1}	0/50/100/150/200
Manganese Mn^{2+}, mg L^{-1}	6
Ammonium NH_4^+, mg L^{-1}	25
Total dissolved solids TDS, g L^{-1} NaCl	0/0.5/1.0/2.0
Sodium* Na^+, mg L^{-1}	11
Calcium* Ca^{2+}, mg L^{-1}	110
Magnesium* Mg^{2+}, mg L^{-1}	9.7
Chloride* Cl^-, mg L^{-1}	23
Phosphate* PO_4^{3-}, mg L^{-1}	0.01
Sulphate* SO_4^{2-}, mg L^{-1}	50
Bicarbonate* HCO_3^-, mg L^{-1}	320

*Average tap water quality: yearly average of water supply system (Stadtwerke Karlsruhe, 2018).

Table 2
Operational parameters MCDI for mode A (energy-efficient) and mode B (high removal)

Phase	Cycle	Mode A (energy-efficient)			Mode B (high removal)		
		Flow rate (L min^{-1})	Cycle time (s)	Applied current (A)	Flow rate (L min^{-1})	Cycle time (s)	Applied current (A)
1	Discharge	0.25	115	57.6	0.25	115	57.6
2	Pre-charge*	1.0	40	18.1	0.25/0.5/0.75/1.0	40	18.1/36/45
3	Charge	1.0	310	18.1	0.25/0.5/0.75/1.0	310	18.1/36/45

*Pre-phase to ensure water quality at beginning of charge cycle

energy consumption SEC (in kWh m^{-3}) were calculated as shown in Eq. (1), considering the electrode module only.

$$\mathrm{SEC} = \frac{E_{\mathrm{module}}}{V_{\mathrm{diluate}}} = \frac{U_{\mathrm{module}} \cdot I_{\mathrm{module}} \cdot t_{\mathrm{experiment}}}{t_{\mathrm{experiment}} \cdot \dot{V}_{\mathrm{diluate}}} \tag{1}$$

The power consumption of the module P_{module} was calculated with the applied potential U (V) and electrical current I (A), which were measured every second. The volume of diluate V (m^3) was calculated at the end of each experiment with the average volume flow $\dot{V}_{\mathrm{diluate}}$ of the diluate phase.

3. Results and discussion

3.1. Arsenic removal

Experiments with model water including sodium chloride (NaCl) (0–1 g L^{-1}) and incremental As(V) concentrations (0.05–0.2 mg L^{-1}) were conducted to examine the specific As removal efficiency of the MCDI unit.

The results for experiments with 0.5 g L^{-1} NaCl are illustrated in Fig. 1 showing a constant average TDS removal of 95.7% ± 1% while only 70.6% ± 3% As-removal was achieved. For all experiments carried out, the electrosorption affinity for As(V) during the charge phase was lower than for chloride (Cl$^-$) achieving an average As selective removal of 80.1% ± 1% from the total TDS rejection. The adsorption behavior of different ions in aqueous solutions by electrical fields can be described by the ion selectivity. Ions compete with each other in the different electrosorption processes leading to different electrosorption capacities. For ions with the same charge, as in the case of As(V) ($H_2AsO_4^-$) and Cl$^-$, ion permeability towards the electrodes tends to increase as the hydrated radius decreases. The better ion selectivity of chloride vs. arsenate is given by its smaller hydrated radius of chloride (Cl$^-$ = 311 pm; As(V) = 340 pm) [17,18]. A slightly better As(V) removal efficiency toward higher As concentrations were observed, increasing from 66% to 74% at 50 and 200 µg L^{-1}, respectively (Fig. 1). With higher bulk ionic concentration, the higher concentration gradient in the electrode macropores acts as a stronger driving force improving the overall adsorption selectivity onto the charging electrical double layer (EDL). These results indicate that the mass of adsorbed ions is dependent not only on the electrosorption kinetics given by the hydrated radius and ionic charge but also on the diffusion coefficient in the macro- and micropores.

To investigate the removal of As on model water simulating real conditions, experiments with tap water were carried out. By changing the model water matrix from NaCl to tap water, higher average As removal rates of 80% ± 3% were achieved while the TDS removal remained constant at about 94% ± 1%. The better As removal with the experiments with tap water is also explained by the lower initial electric conductivity from 1,030 to 670 µS cm^{-1} when using tap water instead of NaCl model water. Ions typically present in tap water seemed to have no negative influence on the As removal at given concentrations (Table 1).

The adsorption behavior of As observed during the experiments with the up-scale unit is in line with previous research on electroselectivity of CDI electrodes. On lab-scale experiments, Hou and Huang [19] and Mossad and Zou [20] showed that the electrosorption capacity onto charged electrodes is dependent on the ionic charge and the hydrated radius of the dissolved ions, as well as the initial feed concentration. Fan et al. [21] demonstrated the electroselectivity of As in comparison to other anions showing lower adsorption as follows: $NO_3^- > F^- > Cl^- >$ As, which is in line with the As removal results of these experiments and results documented in the literature [21–23]. Similar results were observed in laboratory experiments with multi-ionic solutions in different studies that suggested that the higher the ion concentration in the bulk, the greater the adsorption on the activated carbon electrodes [23,24]. By understanding the specific interactions of As within the electrodes, we can corroborate the adsorption behavior for As not only taking into consideration the diffusion and transport models within an electrode cell, but also within the unit module at pilot-scale.

However, results show that the specific As adsorption is strongly inhibited in brackish solution by the higher electroselectivity towards Cl$^-$. The achieved removal efficiency by the MCDI unit was lower than the minimum required for complying with the drinking water standard of 0.01 mg L^{-1}. Achieving concentrations below the standard limit were only possible for concentrations under 50 µg L^{-1} at the given conditions (79% removal) with the chosen MCDI parameters (mode A). The average specific energy demand of the electrode module (in kWh per permeate volume) for the treatment of As was 0.86 ± 0.01 kWh m^{-3} for the experiments with arsenic-spiked tap water and 0.91 ± 0.1 kWh m^{-3} with synthetic water and 0.5 g L^{-1} NaCl.

A low energy consumption was also shown by Fan et al. [21], where removals of >80% were also achieved but with

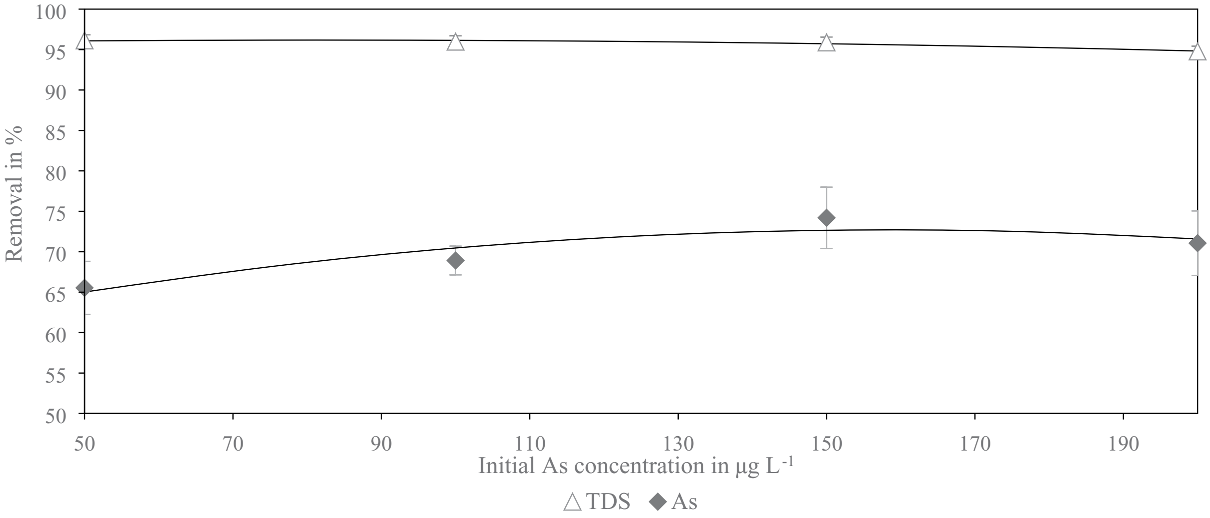

Fig. 1. Removal of As with pilot-scale MCDI (TDS = 0.5 g L^{-1} NaCl, initial pH = 6.5 ± 0.5, and T = 18°C ± 0.2°C).

much higher arsenic concentrations (50 mg L^{-1}), which suggests that operational parameters for the single-pass experiments chosen can still be improved. In order to assess the overall feasibility for As removal with the MCDI unit, its performance was investigated under different conditions and changing operational parameters such as pH, flow rate, and applied current.

3.1.1. Effect of pH

Arsenic electrosorption by CDI results from the electrostatic interaction between arsenate and the carbon electrode surface. Due to the occurrence of different ionic species of As in groundwater, the removal of arsenite As(III) (present as uncharged H_3AsO_3 at neutral pH) with MCDI can be achieved by the oxidation to arsenate As(V) (charged anion) [21]. Likewise, the speciation of As(V) in water is pH dependant, as arsenate might exist as a monovalent or bivalent ion around neutral pH. Experiments with model water spiked with arsenate As(V) at different pH values were carried out showing that the removal efficiency was highly dependent on the ionic state of As. Experiments at pH < pK_a of 6.94 (pH = 6.6 ± 0.1) showed removal rates for monovalent $H_2AsO_4^-$ as low as 30% for the highest volume flows. By slightly increasing the solution pH above the pK_a (pH = 7.2 ± 0.3) the removal of total arsenic increased up to 90%, showing that bivalent arsenate ($HAsO_4^{2-}$) can be more easily electrosorbed by the MCDI. These results are shown in Fig. 2a.

3.1.2. Effect of flow rate

In order to test other options for reducing the As concentration on diluate, experiments with different operational settings of the MCDI module (Table 2, mode B) were carried out. By lowering the flow rate during the charge phase from 1.0 to 0.25 L min^{-1}, a continuous increase in the As removal was achieved. However, there were lower recovery rates (decrease from 82% to 58%) and overall higher specific energy demands. Results are shown in Figs. 2a and b, respectively.

As diluate flow rate decreases, the lower recovery rates (decrease from >80% to <60%) with the constant energy consumption have a direct increase on the specific energy demand from 0.8 to >2.7 kWh m^{-3}. The linear decrease (r^2 = 0.952) of the specific energy demand dependent on the recovery rate (permeate to influent) is shown in Fig. 2b.

3.1.3. Effect of applied current

Following the EDL, electrosorption theory, increased electrical currents during the charge and pre-charge phases (18.1, 36, and 45 A) delivered higher removal efficiencies. However, by increasing the charge current, only the overall salt rejection was improved (94.5% ± 0.7% to 98.1% ± 1%) while the specific As ion removal remained almost equal at 79% ± 2%, as shown in Fig. 3. In a simple EDL model, the condensed layer of counter-ions directly compensates the surface charge on the electrodes. The charge that is hereby being transferred is related to both the electronic charge in the carbon electrode and the ionic charge of the aqueous phase. When applying higher currents to the CDI module, the storage capacity on the electrodes increases as the charge being transferred from one electrode to another is larger and higher ion concentration inside the porous electrodes (EDL) can be stored.

Due to the higher electroselectivity of Cl^- over As(V) the increase in current allowed higher sodium chloride rejection and an overall increase in TDS removal. The charge efficiency Λ in the three experiment series increased slightly with higher applied current from 66.5% to 68.6%. However, specific adsorption capacity for As did not improve during these experiments, while the energy demand increased from 0.86 to 0.89 and 1.44 kWh m^{-3} for the higher applied currents of 18.1, 36 and 45 A, respectively. Correlations in charge efficiency and the adsorption capacity suggest that both internal resistances and diffusion rates control the specific ion adsorption efficiency and increases in current will have a larger effect on the electroselectivity of the species with higher diffusion coefficients.

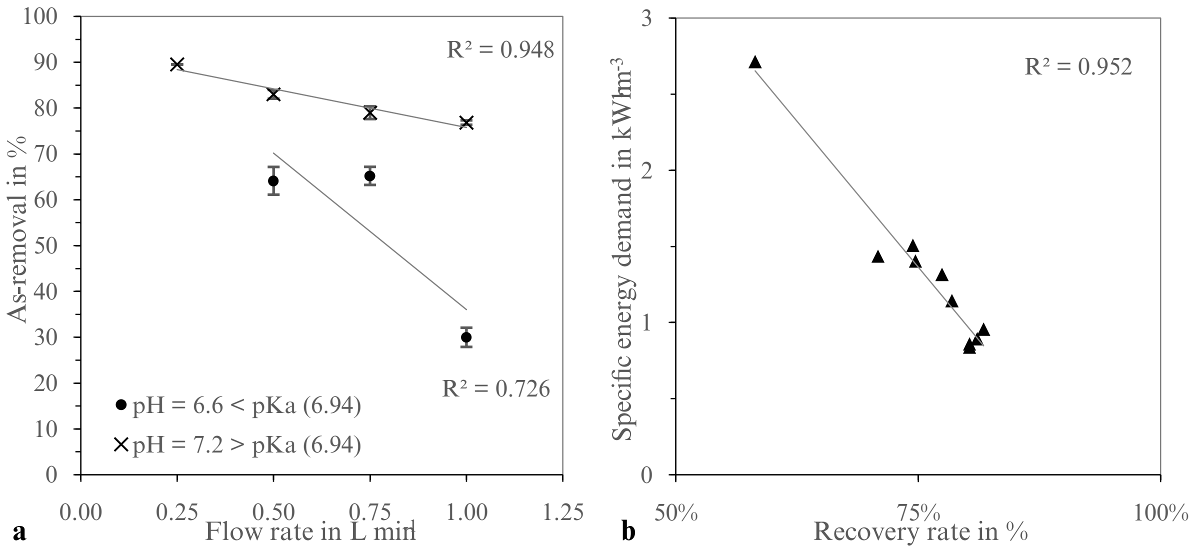

Fig. 2. (a) Decrease in As removal efficiency with higher flow rates and (b) specific energy demand to recovery rate for experiments in mode B.

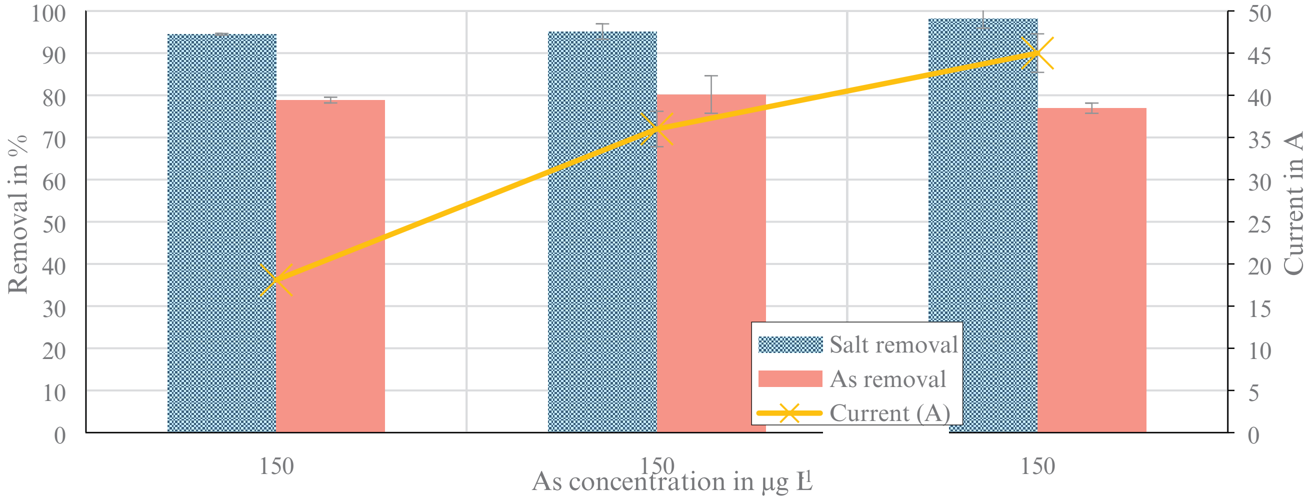

Fig. 3. Removal of 150 µg L^{-1} As in tap water at different applied currents for charge and pre-charge phases (yellow line; 18, 36, and 45 A). Initial pH = 7.0 ± 0.1, temperature = 28.6°C ± 0.3°C.

3.2. Ammonium and manganese removal

3.2.1. Effect of initial concentration

Experiments for Mn^{2+} and NH_4^+ as co-ions in brackish model water with concentrations based on typical values in groundwater in South East Asia (NH_4^+ = 25 mg L^{-1}; Mn^{2+} = 6 mg L^{-1}) were carried out to investigate the specific ion removal capacity of MCDI. The results for the experiments with different initial concentration of sodium chloride (NaCl = 0–2.0 g L^{-1}) are shown in Fig. 4: The decrease in the Mn^{2+} and NH_4^+ removal capacity with increasing TDS (NaCl) concentrations from 99.3% to 32.4% for NH_4^+ and from 100% to 52.6% for Mn^{2+} can be attributed to the electrosorption competition by Na^+ ions. This is in accordance with previously described electrosorption behavior with arsenate (e.g., section 3.1 (Arsenic removal)).

Results also show that the removal efficiency of Mn^{2+} is greater than NH_4^+ and the overall TDS removal (Na^+Cl^-), which can be explained by the higher ionic charge of Mn^{2+} over NH_4^+ and Na^+. The higher removal of NH_4^+ over the Na^+ might be due to its smaller hydrated ion radius (NH_4^+ = 250 pm, Na^+ = 450 pm) [25], which allows a higher ion mobility and increased diffusion towards the electrodes and through the IEM. Better electrosorption of NH_4^+ over Na^+ can be explained as well by its higher initial concentration, which improves the relative sorption performance as seen in the experiments with As and in previous studies [19,22,26,27].

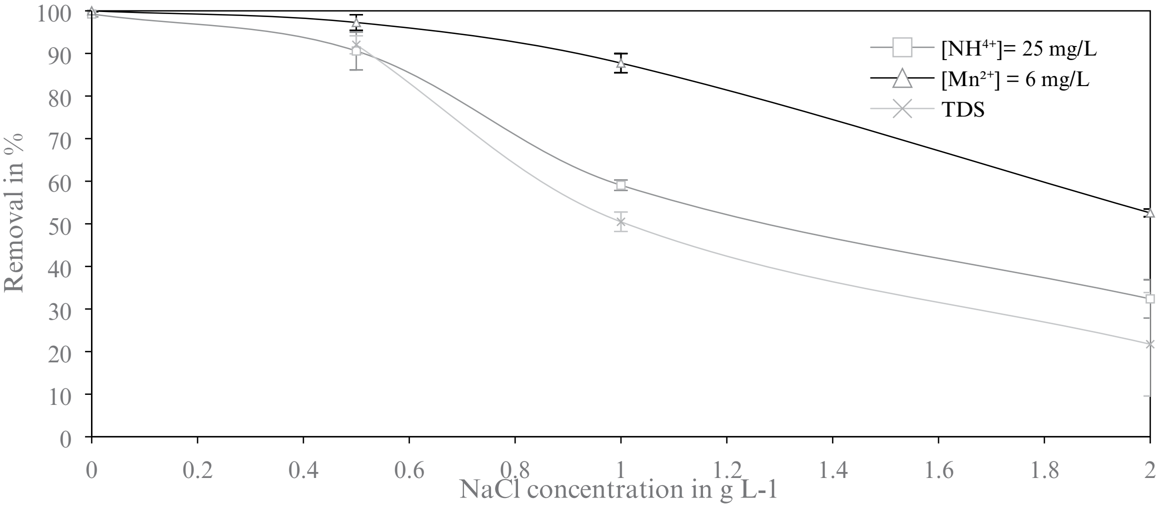

Fig. 4. Removal of manganese ($C_{0,\mathrm{Mn}}$ = 6 mg L^{-1}), ammonium ($C_{0,\mathrm{NH4+}}$ = 25 mg L^{-1}), and total dissolved solids (TDS) with respect to their initial concentrations C_0 vs. increasing initial NaCl. Initial pH = 7.1 ± 0.6 and temperature = 25°C ± 3°C.

Furthermore, the investigation of adsorption competition of similar ions in multi-ionic solutions was carried out with experiments with NH_4^+ and potassium (K^+) using synthetic water spiked with KCl instead of NaCl. As discussed before, adsorption kinetics is characterized by ion mobility, which is given by the charge and hydrated radius of an ionic species. Due to the similarity of NH_4^+ and K^+ with regard to ion mobility (73.4 and 73.5 S cm^2 mol^{-1}, respectively) their adsorption rates are also expected to be very similar. Analog experiments with 25.0 mg L^{-1} NH_4^+ and increasing KCl concentration showed the same removal for both K^+ and NH_4^+ of 97.8% ± 1.2%, 62.7% ± 1.3%, and 44.3% ± 0.9% for 0.5, 1.0, and 2.0 g L^{-1} NaCl, respectively. Thus, the adsorption series for monovalent ions $K^+ \approx NH_4^+ > Na^+$ can be proposed, which follows the behavior of higher sorption with higher ion mobility. For ions with the same charge, higher initial concentration also has an impact on the removal selectivity, as the bulk concentration gradient serves as a driving force for enhanced mobility towards the electrodes and faster electrosorption. Results also show that lower hydrated radius size and higher ionic charge have a positive impact on the removal efficiency due to increased ion mobility. The experiments conducted in this project were able to successfully correlate removal efficiency and ion mobility in a qualitative manner to describe the selectivity of CDI in a pilot scale.

3.2.2. Effect of pH

Because of its dissociation in water, ammonium is present in basic milieus as ammonia (NH_3) which reacts as a weak acid in water (pK_a = 9.2) [28]. In order to investigate how the removal of ammonium is influenced by the pH value, tests were carried out with the feed water at pH = 9.5 ± 0.3. Results show a removal of 97.7% ± 0.3% at an initial ammonium concentration of 17.4 ± 4.4 mg L^{-1}. At strong basic conditions ammonia is the predominant species. High removal rates of NH_3, even though it is not charged, can be explained by pH changes taking place at the electrode level. During the charge phase, a pH change can occur between feed and effluent due to the different adsorption rates of OH^- and H^+.

Dykstra et al. [29] suggests that high pH changes are caused mainly by Faradaic reactions in the micropores by taking the water reduction reaction $2\ H_2O + 2e^- \rightarrow H_{2(g)} + 2\ OH^-$ into consideration, which leads to a pH increase during the charging phase and a decrease during discharging phase. With the higher mobility of OH^- ions, the pH changes to the acidic milieu, shifting the equilibrium to the side of ammonium improving the removal efficiency [29].

4. Conclusions

The selective arsenate (As(V)) electrosorption with MCDI was limited (<89% removal) for the low concentrations given (<0.2 mg L^{-1}) when dissolved salts were present, even at low NaCl concentrations of 0.5 g L^{-1}. This means that complying with the stringent drinking water limit of 0.01 mg L^{-1} was not always possible. The decrease in the As(V), Mn^{2+}, and NH_4^+ removal efficiency with increasing TDS concentrations can be attributed to the electrosorption competition by Cl^- and Na^+ ions.

The removal of NH_4^+ and Mn^{2+} at given concentrations was significantly higher than for As(V) but rejection of As(V) could be tripled by increasing the initial pH value ($pH > pK_{a,As} = 6.94$). A pH value above 7.0 is required for the removal of As(V) with MCDI. However, the selective removal of substances at very low concentrations (µg-range) is mostly limited by the TDS concentration of the raw water.

In general, MCDI represents a viable option for the removal of Mn^{2+} and NH_4^+ from contaminated brackish water with an optimal energy consumption below <1 kWh m^3, depending on selected operational settings and feed water characteristics. However, removal efficiency can drop by half when feed TDS concentration is doubled from 1 to 2 g L^{-1}. In order to improve removal efficiency at higher TDS, higher currents (increased energy consumption >1 kWh) and shorter charge cycles (lower recovery < 60%) should be considered. For the removal of arsenic in brackish water with competing ions, further tests with substances such as phosphate, silica, and carbonates must be carried out.

Acknowledgments

This study was carried out within the joint research project WaKap with the financial aid of the German Federal Ministry of Education and Research (BMBF) under grant number 02WAV1413A.

References

[1] S. Dasgupta, F. Akhter, K. Zahirul, Z. Khan, S. Choudhury, A. Nishat, River Salinity and Climate Change Evidence from Coastal Bangladesh, 2014. Available at: http://econ.worldbank.org (accessed August 23, 2018).

[2] D. Wheeler, Quantifying Vulnerability to Climate Change: Implications for Adaptation Assistance, Washington DC, 2011. Available at: http://www.cgdev.org/content/publications/detail/1424759 (accessed August 24, 2018).

[3] L.H.E. Winkel, P.T.K. Trang, V.M. Lan, C. Stengel, M. Amini, N.T. Ha, P.H. Viet, M. Berg, Arsenic pollution of groundwater in Vietnam exacerbated by deep aquifer exploitation for more than a century, Proc. Natl. Acad. Sci. U.S.A., 108 (2011) 1246–1251.

[4] D. Chakraborti, M.M. Rahman, A. Mukherjee, M. Alauddin, M. Hassan, R.N. Dutta, S. Pati, S.C. Mukherjee, S. Roy, Q. Quamruzzman, M. Rahman, S. Morshed, T. Islam, S. Sorif, M. Selim, M.R. Islam, M.M. Hossain, Groundwater arsenic contamination in Bangladesh—21 years of research, J. Trace Elem. Med. Biol., 31 (2015) 237–248.

[5] S. Bhowmick, S. Pramanik, P. Singh, P. Mondal, D. Chatterjee, J. Nriagu, Arsenic in groundwater of West Bengal, India: a review of human health risks and assessment of possible intervention options, Sci. Total Environ., 612 (2018) 148–169.

[6] D. Chakraborti, M.M. Rahman, B. Das, M. Murrill, S. Dey, S. Chandra Mukherjee, R.K. Dhar, B.K. Biswas, U.K. Chowdhury, S. Roy, S. Sorif, M. Selim, M. Rahman, Q. Quamruzzaman, Status of groundwater arsenic contamination in Bangladesh: a 14-year study report, Water Res., 44 (2010) 5789–5802.

[7] L. Zhang, X. Qin, J. Tang, W. Liu, H. Yang, Review of arsenic geochemical characteristics and its significance on arsenic pollution studies in karst groundwater, Southwest China, Appl. Geochem., 77 (2017) 80–88.

[8] A. Sarkar, B. Paul, The global menace of arsenic and its conventional remediation - a critical review, Chemosphere, 158 (2016) 37–49.

[9] M. Amini, K.C. Abbaspour, M. Berg, L. Winkel, S.J. Hug, E. Hoehn, H. Yang, C.A. Johnson, Statistical modeling of global geogenic arsenic contamination in groundwater, Environ. Sci. Technol., 42 (2008) 3669–3675.

[10] M. Berg, C. Stengel, P.T.K. Trang, P. Hung Viet, M.L. Sampson, M. Leng, S. Samreth, D. Fredericks, Magnitude of arsenic pollution in the Mekong and Red River Deltas - Cambodia and Vietnam, Sci. Total Environ., 372 (2007) 413–425.

[11] K.M. Campbell, D.K. Nordstrom, Arsenic speciation and sorption in natural environments, Rev. Mineral. Geochem., 79 (2014) 185–216.

[12] J. Norrman, C.J. Sparrenbom, M. Berg, D.N. Dang, G. Jacks, P. Harms-Ringdahl, Q.N. Pham, H. Rosqvist, Tracing sources of ammonium in reducing groundwater in a well field in Hanoi (Vietnam) by means of stable nitrogen isotope (δ15N) values, Appl. Geochem., 61 (2015) 248–258.

[13] Y. Jia, B. Xi, Y. Jiang, H. Guo, Y. Yang, X. Lian, S. Han, Distribution, formation and human-induced evolution of geogenic contaminated groundwater in China: a review, Sci. Total Environ., 643 (2018) 967–993.

[14] S. Datta, K. Johannesson, N. Mladenov, M. Sankar, S. Ford, M. Vega, A. Neal, M. Kibria, A. Krehel, G. Hettiarachchi, Groundwater-Sediment Sorption Mechanisms and Role of Organic Matter in Controlling Arsenic Release into Aquifer Sediments of Murshidabad Area (Bengal basin), India, Proceedings of the 5th International Congress on Arsenic in the Environment, May 11-16, 2014, Buenos Aires, Argentina, In: One Century of the Discovery of Arsenicosis in Latin America (1914–2014) As 2014, Taylor & Francis, London, 2014, pp. 95–97.

[15] M. Berg, P.T.K. Trang, C. Stengel, J. Buschmann, P.H. Viet, N. Van Dan, W. Giger, D. Stüben, Hydrological and sedimentary controls leading to arsenic contamination of groundwater in the Hanoi area, Vietnam: the impact of iron-arsenic ratios, peat, river bank deposits, and excessive groundwater abstraction, Chem. Geol., 249 (2008) 91–112.

[16] E.E. Cañas Kurz, V.T. Luong, U. Hellriegel, F. Leidinger, T.L. Luu, J. Bundschuh, J. Hoinkis, Iron-based subsurface arsenic removal (SAR): results of a long-term pilot-scale test in Vietnam, Water Res., 181 (2020) 115929, https://doi.org/10.1016/j.watres.2020.115929.

[17] A.G. Volkov, D.W. Deamer, Liquid-Liquid Interfaces: Theory and Methods, CRC Press, 1996. Available at: https://www.crcpress.com/Liquid-Liquid-InterfacesTheory-and-Methods/Volkov-Deamer/p/book/9780849376948 (accessed August 28, 2018).

[18] J. Mähler, I. Persson, R.B. Herbert, Hydration of arsenic oxyacid species, Dalton Trans., 42 (2013) 1364–1377.

[19] C.-H. Hou, C.-Y. Huang, A comparative study of electrosorption selectivity of ions by activated carbon electrodes in capacitive deionization, Desalination, 314 (2013) 124–129.

[20] M. Mossad, L. Zou, A study of the capacitive deionisation performance under various operational conditions, J. Hazard. Mater., 213–214 (2012) 491–497.

[21] C.-S. Fan, S.-C. Tseng, K.-C. Li, C.-H. Hou, Electro-removal of arsenic(III) and arsenic(V) from aqueous solutions by capacitive deionization, J. Hazard. Mater., 312 (2016) 208–215.

[22] Z. Chen, H. Zhang, C. Wu, Y. Wang, W. Li, A study of electrosorption selectivity of anions by activated carbon electrodes in capacitive deionization, Desalination, 369 (2015) 46–50.

[23] Y. Li, C. Zhang, Y. Jiang, T.J. Wang, H. Wang, Effects of the hydration ratio on the electrosorption selectivity of ions during capacitive deionization, Desalination, 399 (2016) 171–177.

[24] P. Xu, J.E. Drewes, D. Heil, G. Wang, Treatment of brackish produced water using carbon aerogel-based capacitive deionization technology, Water Res., 42 (2008) 2605–2617.

[25] J. Kielland, Individual activity coefficients of ions in aqueous solutions, J. Am. Chem. Soc., 59 (1937) 1675–1678.

[26] C.J. Gabelich, T.D. Tran, I.H. Mel Suffet, Electrosorption of inorganic salts from aqueous solution using carbon aerogels, Environ. Sci. Technol., 36 (2002) 3010–3019.

[27] R. Zhao, M. van Soestbergen, H.H.M. Rijnaarts, A. van der Wal, M.Z. Bazant, P.M. Biesheuvel, Time-dependent ion selectivity in capacitive charging of porous electrodes, J. Colloid Interface Sci., 384 (2012) 38–44.

[28] J.M. Hales, D.R. Drewes, Solubility of ammonia in water at low concentrations, Atmos. Environ., 13 (1979) 1133–1147.

[29] J.E. Dykstra, K.J. Keesman, P.M. Biesheuvel, A. van der Wal, Theory of pH changes in water desalination by capacitive deionization, Water Res., 119 (2017) 178–186.